NEOPLASIA
www.neoplasia.com

Volume 15 Number 6 June 2013 pp. 591–599 591

Combination of Oncolytic Herpes Simplex Viruses Armed with Angiostatin and IL-12 Enhances Antitumor Efficacy in Human Glioblastoma Models[1]

Wei Zhang*,†, Giulia Fulci*, Hiroaki Wakimoto*, Tooba A. Cheema*, Jason S. Buhrman*, Deva S. Jeyaretna‡, Anat O. Stemmer Rachamimov§, Samuel D. Rabkin* and Robert L. Martuza*

*Brain Tumor Research Center, Molecular Neurosurgery Laboratory, Department of Neurosurgery, Massachusetts General Hospital, Boston, MA; †Department of Neurosurgery, Xijing Hospital, The Fourth Military Medical University, Xi'an, Shaanxi Province, People's Republic of China; ‡Department of Neurosurgery, Frenchay Hospital, Bristol, United Kingdom; §Department of Pathology, Massachusetts General Hospital, Boston, MA

Abstract

Oncolytic herpes simplex virus (oHSV) can potentially spread throughout the tumor, reach isolated infiltrating cells, kill them, and deliver anticancer agents. However, the host responds to oHSV by inducing intratumoral infiltration of macrophages that can engulf the virus, limiting the potential of this therapeutic strategy. Hypervascularity is a pathognomonic feature of glioblastoma (GBM) and is a promising therapeutic target. Antiangiogenic treatments have multiple benefits, including the capacity to increase oHSV efficacy by suppressing macrophage extravasation and infiltration into the tumor. Angiostatin is an antiangiogenic polypeptide, and interleukin-12 (IL-12) is an immunostimulatory cytokine with strong antiangiogenic effects. Clinical use of each has been limited by delivery issues and systemic toxicity. We tested a combination treatment strategy using oHSVs expressing angiostatin (G47Δ-mAngio) and IL-12 (G47Δ-mIL12) in two orthotopic human GBM models. Intratumoral injection of G47Δ-mAngio and G47Δ-mIL12 in mice bearing intracranial U87 or tumors derived from glioblastoma stem cells significantly prolonged survival compared to each armed oHSV alone. This was associated with increased antiangiogenesis and virus spread and decreased macrophages. These data support the paradigm of using oHSV expressing different antiangiogenic agents and show for the first time that oHSVs expressing angiostatin and IL-12 can improve efficacy in human GBM models.

Neoplasia (2013) 15, 591–599

Introduction

Despite improved understanding of the molecular and physiological features of glioblastoma (GBM), there are no curative treatments for this brain cancer. Several modalities have been and continue to be tested to treat these tumors, but none of these can extend life for more than a few additional months. The median life expectancy after diagnosis remains approximately 15 months [1]. Genetically engineered oncolytic herpes simplex virus (oHSV) is an attractive cancer therapeutic due to its capacity to selectively replicate in cancer cells, kill them, and spread their progeny to additional cancer cells [2,3]. Moreover, the mode by which oHSV kills tumor cells differs from that of standard anticancer agents and has a differing set of potential toxicities, thus making oHSV useful for multimodal combination treatments [4–7]. In addition to their oncolytic action, oHSVs can be "armed" to express therapeutic transgenes [3,8].

Despite the biologic rationale, the efficacy of unarmed oHSV in the clinic for brain tumors has been limited so far. Recent studies have shown that tumor-associated macrophages and microglia limit the replication and spread of oHSV and other oncolytic viruses [9–13].

Abbreviations: GBM, glioblastoma; oHSV, oncolytic herpes simplex virus; GSCs, glioblastoma stem cells; IHC, immunohistochemistry; HUVECs, human umbilical vein endothelial cells; IL-12, interleukin-12; VEGF, vascular endothelial growth factor; EGFR, epidermal growth factor receptor; pfu, plaque-forming units

Address all correspondence to: Robert L. Martuza, MD, GB502, Massachusetts General Hospital, 55 Fruit St., Boston, MA 02114. E-mail: rmartuza@partners.org

[1]This study was supported in part through grant NS032677 from the National Institutes of Health and the Rendina Family Foundation to R.L.M. and the National Natural Science Foundation of China (No. 81171087) to W.Z.

Received 8 January 2013; Revised 23 March 2013; Accepted 25 March 2013

DOI 10.1593/neo.13158

Antiangiogenic therapy is one of the newer strategies being pursued to treat GBM. However, the only antiangiogenic drug that has been approved for recurrent GBM, bevacizumab, presents only palliative effects [14,15]. It is thus important to develop new strategies that will improve the efficacy and safety of this treatment modality. Several endogenous proteins that have antiangiogenic activity and oHSVs have been identified. Thus, oHSVs armed with antiangiogenic factors may result in significant improvement of GBM treatment, as they combine oncolytic and antiangiogenic activities [16]. This is further emphasized by recent data showing that antiangiogenic treatments can decrease intratumoral macrophages, which in turn increases replication and spread of oncolytic viruses [12,17–19].

Angiostatin, an internal fragment of plasminogen, induces regression of the tumor vasculature, inhibits cancer cell invasion, and suppresses tumor growth *in vivo*, including in GBM [20–24]. However, because angiostatin has a very short half-life, it presents important delivery problems [25]. A number of replication-defective gene therapy vectors expressing angiostatin have been developed and tested in glioma models [19,26] but have never been tested in patients with GBM. Interleukin-12 (IL-12) is a principal Th1 cytokine with antiangiogenic properties. Its antiangiogenic and antitumor effects were successfully tested when delivered to a mouse squamous cell carcinoma using oHSV as a vector [27]. Of note, IL-12 is a mediator of angiostatin activity; angiostatin is unable to exert angiogenesis inhibition in mice with gene-targeted deletion of either the IL-12–specific receptor subunit IL12Rβ2 or the IL-12 p40 subunit [28]. Moreover, delivery of murine angiostatin and IL-12 by replication-defective adenoviral vectors shrank tumors in an immunocompetent mouse model of breast carcinoma [29]. Therefore, we have hypothesized that a combination of oHSVs armed with angiostatin and IL-12 could improve GBM treatment.

G47Δ [30] is an oHSV currently in clinical trial for GBM patients [31]. We previously described G47Δ-mAngio, G47Δ armed with mouse angiostatin, and showed that it improves survival of mice with established U87 tumors compared to the control vector G47Δ-Empty [19]. In addition, the same study showed that the combination of G47Δ-mAngio with bevacizumab had an additive therapeutic effect and suggested the advantage of combining different antiangiogenic agents with different mechanisms of actions and adverse effects [19]. More recently, a G47Δ vector expressing mouse IL-12 (G47Δ-mIL12) has also been engineered in our laboratory.

To test our hypothesis of combining oHSVs armed with both angiostatin and IL-12, we have used G47Δ-mAngio plus G47Δ-mIL12 to treat two different human intracranial GBM tumor models: one originated from the U87 glioma cell line and the other from MGG4, a cancer stem cell line isolated from a GBM patient surgical specimen [32,33]. In both models, our results demonstrate that the combination of two antiangiogenic agents with different mechanisms of action, each one delivered through an oHSV vector, provides significantly better outcomes against GBM than oHSV expressing either antiangiogenic agent alone.

Materials and Methods

Cell Lines and Cell Culture

U87 human glioma cells were purchased from American Type Culture Collection (ATCC, Manassas, VA) and grown in complete Dulbecco's modified Eagle's medium supplemented with 10% fetal calf serum. Human glioblastoma stem cells (GSCs; MGG4, MGG6, MGG7, MGG8, MGG13, MGG18, MGG23, MGG27, and MGG29) were isolated from resection specimens of newly diagnosed GBM as previously described [32,33]. MGG30 was established from a recurrent GBM. BT74 was obtained from Dr Santosh Kesari (University of California, San Diego, CA) and was originally described as GBM6 in [34]. Cultures of GSCs were maintained as spheres in serum-free medium containing 20 ng/ml recombinant human epidermal growth factor (R&D Systems, Minneapolis, MN) and 20 ng/ml recombinant human fibroblast growth factor 2 (FGF2; Peprotech, Rocky Hill, NJ). Passaging of the cultures was conducted by dissociating neurospheres using the NeuroCult Chemical Dissociation Kit (StemCell Technologies, Vancouver, Canada). Human umbilical vein endothelial cells (HUVECs) were purchased from Lonza/Clonetics (Basel, Switzerland) and grown in EGM-2 medium supplemented with the bullet kit provided by the company, which includes 2% FBS, heparin, hydrocortisone, ascorbic acid, and the following human growth factors: fibroblast, R3-insulin, and vascular endothelial growth factor (VEGF). HUVECs were maintained in culture for no more than 10 passages.

Viruses

The oHSV G47Δ, containing deletions of the *γ34.5* and *α47* genes and an inactivating insertion of *Escherichia coli* LacZ into ICP6 [30], was armed with the mouse angiostatin cDNA tagged with the hemagglutinin epitope (G47Δ-mAngio, [19]) or with mouse IL-12 cDNA (G47Δ-mIL12). Mouse IL-12 cDNA (p35 and p40 separated by two bovine elastin motifs) [35] was cloned into a shuttle vector plasmid, pVec92-fmIL12, and inserted into pG47Δ-BAC using Cre recombinase (New England Biolabs, Ipswich, MA). Recombinant oHSV was isolated as previously described [36].

Endothelial Cell Tube Formation Assay

U87 or MGG4 cells were infected with G47Δ-Empty, G47Δ-mAngio, G47Δ-mIL12, or G47Δ-mAngio+mIL12 (total virus multiplicity of infection = 1) for 12 hours (U87 cells) or 24 hours (MGG4 GSCs) using Dulbecco's modified Eagle's medium with 2% fetal calf serum. Infectious virus in the supernatants was blocked by adding 1% pooled human gamma globulin (Gamastan; Grifols Therapeutics, Inc, Barcelona, Spain) 1 hour after infection. This IgG concentration was previously shown to block virus infection of HSV-susceptible cells. The supernatants were then collected and used in the tube assay described below. HUVECs (1×10^5 cells/well) were seeded on matrigel (Matrigel Matrix; BD Biosciences, Franklin Lakes, NJ) precoated 24-well culture plates and grown in EGM-2 medium (negative control) or supernatants collected from virus-infected cells. Tube formation was scored 6 hours later by counting the number of tubular structures made between cells using an inverted microscope (Nikon, Melville, NY; OPTIPHOT-2). Each supernatant was tested in triplicate. Three random fields were chosen for counting.

Animal Studies

Female athymic nu/nu mice aged 6 to 8 weeks were obtained from NCI Frederick (Frederick, MD). To generate intracerebral xenografts, 2×10^4 GSCs or 2×10^5 U87 cells in 2 μl of phosphate-buffered saline (PBS) were stereotactically implanted into the right cerebrum (2 mm lateral to the bregma at a depth of 3 mm) as described [32]. Seven days (U87) or 4 weeks (MGG4) after implantation, 2 μl of virus [1×10^6 plaque-forming units (pfu)] or PBS was injected at the same stereotactic coordinates. When neurologic symptoms became

significant, mice were sacrificed by cardiac perfusion with 4% paraformaldehyde, and the brains removed for histopathologic analysis. All animal procedures were performed with the approval of the Subcommittee on Research Animal Care (SRAC) at Massachusetts General Hospital.

Immunohistochemistry

Brains were frozen in an isopentane–dry ice bath and then sectioned by cryostat to a thickness of 5 μm through the entire tumor volume. Every fifth section was collected for analysis. Tissue slides were dried overnight at room temperature, fixed in ice-cold acetone, and stored at −20°C for hematoxylin and eosin staining and immunohistochemistry (IHC) analysis. The tissue slides were thawed and rehydrated in PBS before staining. Each brain was analyzed for the presence of GBM cells [human epidermal growth factor receptor (EGFR)], vascular density (CD31), macrophage infiltration (F4/80), and VEGF expression as follows: endogenous proteins and peroxidases were blocked with serum-free protein block and peroxidase-blocking reagent (DakoCytomation, Glostrup, Denmark). Mouse IgG was blocked with mouse on mouse reagent (Vector Laboratories, Burlingame, CA). Sections were then incubated overnight at 4°C with each of the following primary antibodies: mouse anti-human EGFR (M3563; Dako), rat anti-mouse CD31 (550274; BD Pharmingen, Franklin Lakes, NJ), rat anti-mouse F4/80 (MCA497RT; Serotec, Kidlington, Oxford, United Kingdom), and mouse anti-human VEGF antibody (555036; BD Biosciences). This was followed by incubation with anti-rat or anti-mouse IgG-HRP secondary antibody (Amersham, Piscataway, NJ). Liquid DAB Substrate Chromogen System (DakoCytomation) was used for detection. To quantify CD31 or VEGF immunopositive areas, NIH ImageJ software assisted with the color deconvolution plugin was used to analyze six randomly chosen high magnification microscopic images per tumor. Intratumoral G47Δ spread was analyzed through staining of viral β-galactosidase activity with X-gal reagent (5-bromo-4-chloro-3-inodolyl-β-D-galactopyranoside; Sigma, St Louis, MO; 0.4 mg/ml in PBS) added to the acetone-fixed slides and incubated at 37°C for 4 hours. In all cases, the sections were counterstained with hematoxylin, dehydrated with increasing concentrations of ethanol, and fixed in xylene. NIH ImageJ software was used to calculate the viral infected area in 10 different tumor sections cut across the whole tumor volume.

Statistical Analysis

Statistical analysis of animal survival was performed with log-rank (Mantel-Cox) test. All other experiments were analyzed with two-sided analysis of variance test followed by means comparisons with post hoc Tukey's test (GraphPad Prism software). $P < .05$ was considered to be statistically significant. All error bars indicate SDs.

Results

Antiangiogenic Effects of Combination G47Δ-mAngio Plus G47Δ-mIL12 Treatment in the U87 Human Glioma Model In Vitro

We first tested the effects of supernatants from U87 cells infected with G47Δ-Empty, G47Δ-mAngio, G47Δ-mIL12, or G47Δ-mAngio

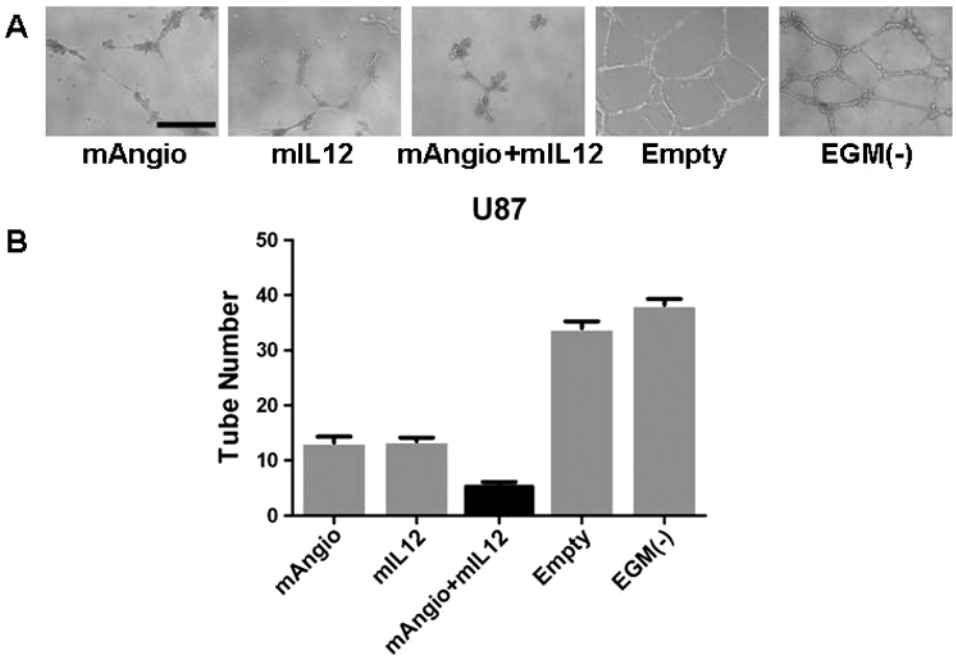

Figure 1. Antiangiogenic effect of supernatants collected from virus-infected U87 cells *in vitro*. (A) Representative images of tubular structures formed by HUVECs when grown on a matrigel substrate with supernatants from infected U87 cells. The bar indicates 0.5 mm. (B) The number of tubes counted when HUVECs were grown in the presence of supernatants from U87 cells infected with G47Δ-Empty (Empty; 35.25 ± 0.85), G47Δ-mAngio (mAngio; 13.25 ± 1.11), G47Δ-mIL12 (mIL12; 13.50 ± 0.65), G47Δ-mAngio + G47Δ-mIL12 (mAngio + mIL12; 5.25 ± 0.85), or EGM (−; 38.25 ± 1.12). The bars indicate average number of tubes ± SD. Statistically significant differences were observed for Empty *versus* mAngio, $P < .0001$; Empty *versus* mIL12, $P < .0001$; mAngio *versus* mAngio + mIL12, $P = .0012$, mIL12 *versus* mAngio + mIL12, $P = .0006$; EGM(−) *versus* mAngio + mIL12, $P < .0001$; EGM(−) *versus* mAngio, $P < .0001$; EGM(−) *versus* mIL12, $P < .0001$.

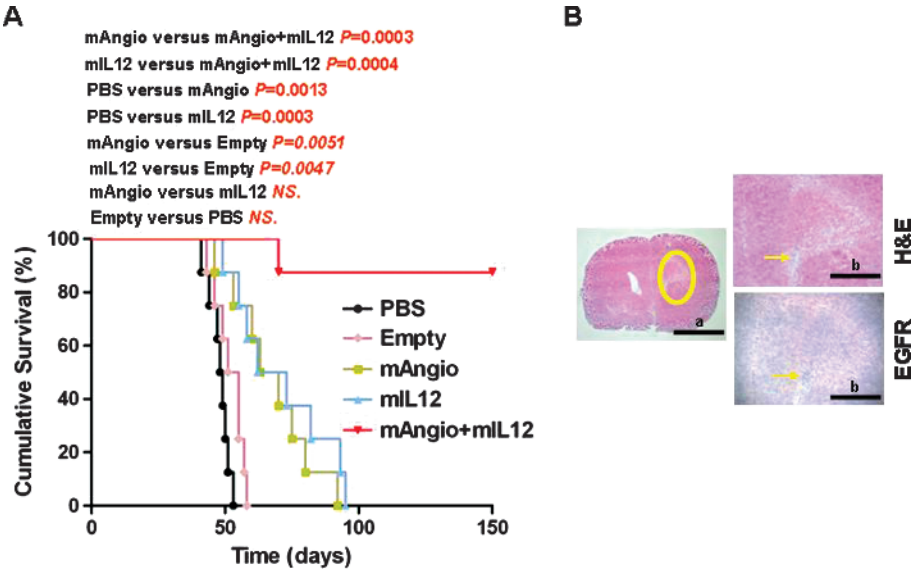

Figure 2. Kaplan-Meier analysis of survival after combination treatment in U87 intracranial glioma model. (A) Survival of mice with established U87 intracranial tumors treated intratumorally with PBS, G47Δ-Empty, G47Δ-mAngio, G47Δ-mIL12, and G47Δ-mAngio + G47Δ-mIL12 (1×10^6 pfu on day 7; $n = 8$/group). The *P* values for each pairwise comparison are indicated. (B) Histopathologic analysis of a representative brain taken from the mAngio + mIL12 treatment group that remained asymptomatic 150 days after tumor implantation. The same section is shown at two different magnifications (bar a indicates 5 mm, and bar b indicates 2 mm). Left panel: The circle indicates the area around the site of tumor implantation. Right upper panel: Hematoxylin and eosin. Right lower panel: EGFR IHC. Arrows indicate area where dispersed cancer cells and inflammation were observed.

plus G47Δ-mIL12 combination (mAngio + mIL12) in a HUVEC tube formation assay *in vitro* (Figure 1*A*). While supernatants from U87 cells infected with either G47Δ-mAngio or G47Δ-mIL12 significantly decreased tube formation *in vitro* compared with control, the combination of the two viruses further inhibited tube formation (Figure 1, *A* and *B*).

G47Δ-mAngio Plus G47Δ-mIL12 Treatment of the U87 Glioma In Vivo

We next determined the therapeutic benefit of G47Δ-mAngio and G47Δ-mIL12 individually and in combination in intracranial U87 gliomas established in athymic mice. Intratumoral injection of each virus alone (1×10^6 pfu) had a significant and similar therapeutic effect and extended median survival from 48 days (PBS) and 53 days (G47Δ-Empty) to 66 (G47Δ-mAngio) and 67 (G47Δ-mIL12) days. The combination of mAngio + mIL12 (0.5×10^6 pfu each) was significantly better than either virus alone, with seven of eight (87.5%) tumor-bearing mice surviving at least 150 days (about three times median survival of PBS; Figure 2*A*). At that point, the surviving mice were sacrificed and the brains were removed for histopathologic analysis, which revealed the presence of only few dispersed tumor cells surrounded by infiltrative neutrophils and macrophages (Figure 2*B*). These results demonstrate a significant therapeutic advantage of using these two oHSVs together in treating orthotopic GBM tumors in mice.

Screening of CD31 and VEGF Expression in Human GSC Xenografts

Although U87 is a highly vascular and commonly used glioma model, it does not present the cellular heterogeneity or histopathologic hallmarks commonly seen in human GBMs; therefore, we sought to test this combination therapy on human GSC-derived tumors, which recapitulate pathologic features of the GBM from which they were isolated. We screened a cohort of GSC intracerebral tumors derived from 11 different GSC lines for $CD31^+$ vessel density and VEGF expression intensity to establish the relative angiogenic levels in each of them (Figure 3). MGG4 demonstrated the highest $CD31^+$ vascularity, characterized by aberrantly tortuous and dilated tumor-associated vasculature (Figure 3*A*), which was associated with strong VEGF immunopositivity within the tumor (Figure 3). Thus, this tumor model was chosen to test the combination mAngio + mIL12 treatment. The expression of $CD31^+$ and VEGF in different GSC lines were quantified (Figure 3*B*).

G47Δ-mAngio Plus G47Δ-mIL12 Treatment of the Human GSC MGG4 Model In Vitro *and* In Vivo

To evaluate the antiangiogenic activity of virus therapy, as with U87, we first tested the effects of supernatants collected from infected MGG4 cells on HUVEC tube formation on matrigel *in vitro* (Figure 4*A*). Supernatants derived from G47Δ-mAngio or G47Δ-mIL12 alone decreased HUVEC tube formation, whereas the combination of mAngio + mIL12 further inhibited tube formation (Figure 4*B*). We then determined the therapeutic benefit of G47Δ-mAngio (mAngio) and G47Δ-mIL12 (mIL12) individually and in combination on intracranial MGG4-derived tumors established in nude mice. G47Δ-mAngio or G47Δ-mIL12 alone had a similar therapeutic benefit in this tumor model and were significantly better than G47Δ-Empty (lacking any therapeutic transgene; Figure 5). In this model, G47Δ-Empty was not any better than PBS, although each armed virus alone was better than PBS or G47Δ-Empty. Importantly, the combination of mAngio + mIL12 significantly extended median survival from 98 days for the groups treated with either PBS or G47Δ-empty to

136 days (Figure 5). Furthermore, mice receiving the combination virus treatment survived significantly longer than those receiving either G47Δ-mAngio or G47Δ-mIL12 alone (Figure 5).

G47Δ Distribution in GSC-Derived Tumors

Antiangiogenic treatments have been shown to increase intratumoral virus distribution by suppressing infiltration of peripheral macrophages [12,17–19]. We therefore examined intratumoral virus distribution through X-gal staining 3 days after virus injection (Figure 6) and evaluated intratumoral levels of angiogenesis (VEGF and CD31 markers) and macrophages (F4/80) in the same tumors by IHC (Figure 7). Three days after virus injection is the earliest time point when, in the absence of adjuvant therapy, oHSV oncolytic activity is completely suppressed [10] (Figure 6). Indeed, reduction of virus-induced intratumoral macrophages was shown to be associated with increased viral spread [11].

To quantify LacZ expression inside the tumor, we used human EGFR staining to localize tumor and calculated the percentage of tumor area stained with X-gal (Figure 6). G47Δ-Empty exhibited only a small area of infected tumor cells (Figure 6). In contrast, G47Δ-mAngio and G47Δ-mIL12 had more extensive intratumoral virus distribution. Combination treatment further increased virus distribution, which was dispersed through more than 50% of the tumor (Figure 6*B*). Therefore, increased efficacy of the combined G47Δ-mAngio + G47Δ-mIL12 treatment was associated with increased virus spread.

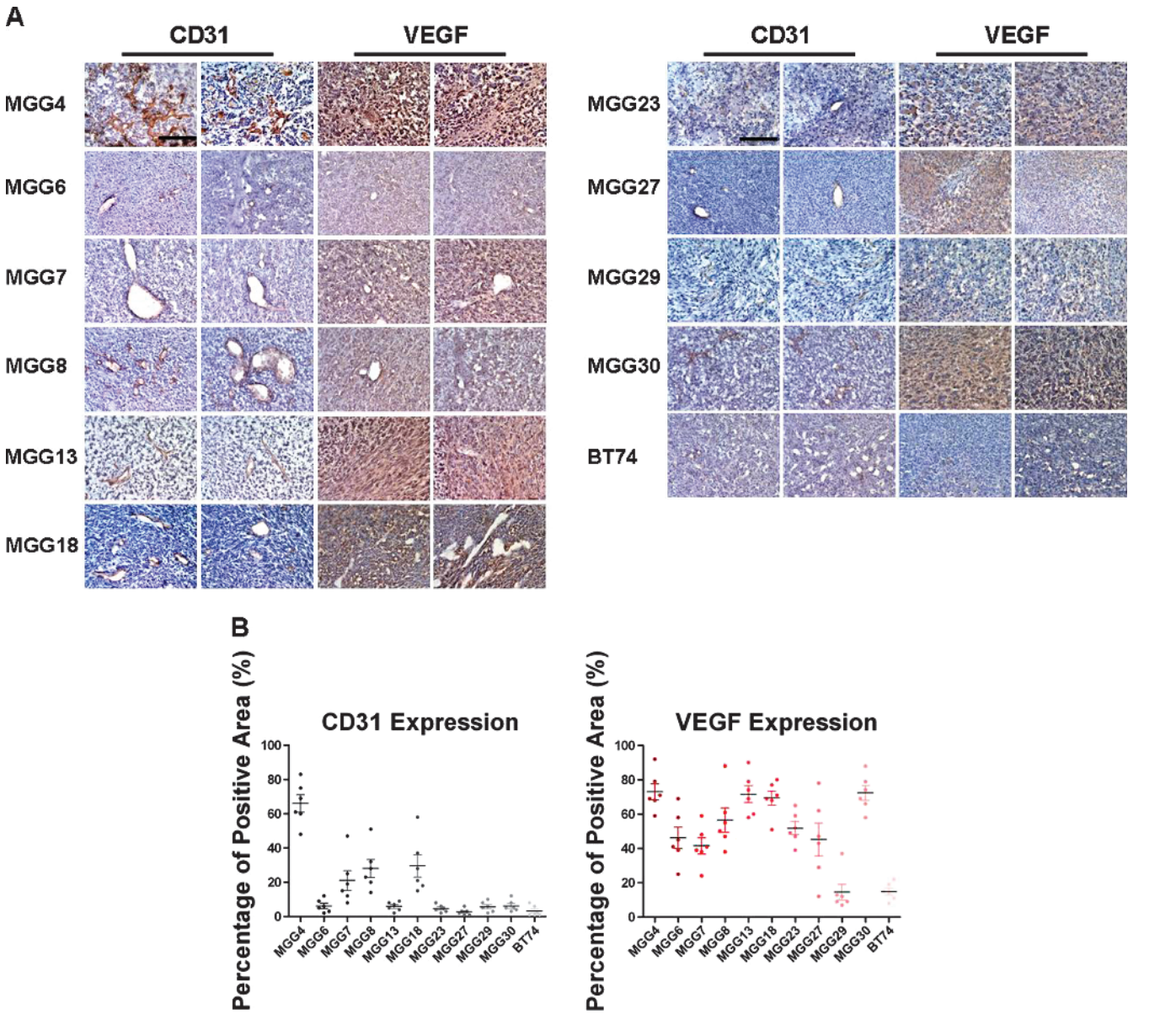

Figure 3. Immunohistochemical analysis of vascularity in human GSC xenografts. (A) Sections of the central tumor show tumor vascularity (CD31, brown) and VEGF expression (VEGF, diffuse brown staining of the secreted molecule) from human GSCs: MGG4, MGG6, MGG7, MGG8, MGG13, MGG18, MGG23, MGG27, MGG29, MGG30, and BT74. Two representative fields from different areas of the same tumors are shown for each protein. The bar indicates 0.5 mm. (B) The graphs show the percentage of area positive for CD31 or VEGF expression. The bars indicate the average percentage of positive areas from six independent fields ± SD.

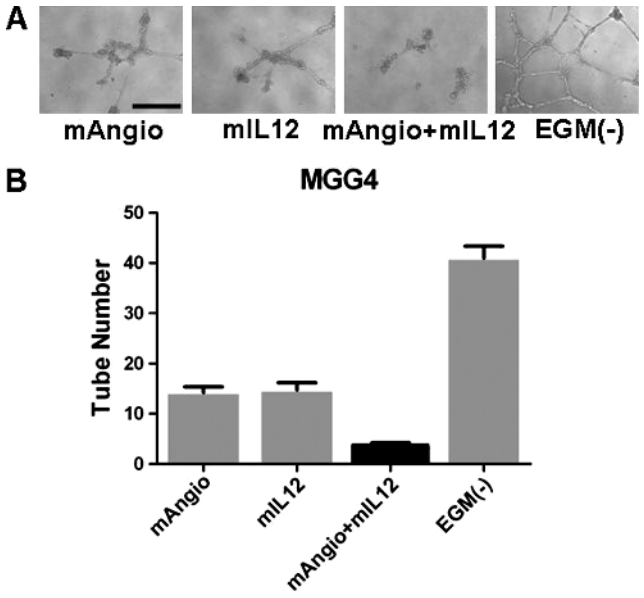

Figure 4. Antiangiogenic effects of supernatants collected from virus-infected MGG4 GSCs *in vitro*. (A) Representative tubular structures formed by HUVECs when grown on a matrigel substrate with supernatants from infected MGG4 GSCs. The bar indicates 0.5 mm. (B) The number of tubes counted when HUVECs were grown in the presence of supernatants from MGG4 GSCs infected with G47Δ-mAngio (mAngio; 14.25 ± 1.11 tubes), G47Δ-mIL12 (mIL12; 14.75 ± 1.44 tubes), G47Δ-mAngio + G47Δ-mIL12 (mAngio + mIL12; 3.75 ± 0.48 tubes), or EGM (−; 41 ± 2.35 tubes). The bars indicate average number of tubes ± SD. Statistically significant differences were observed for mAngio *versus* mAngio + mIL12, $P < .0001$; mIL12 *versus* mAngio + mIL12, $P = .0003$; EGM(−) *versus* mAngio + mIL12, $P < .0001$; EGM(−) *versus* mAngio, $P < .0001$; and EGM(−) *versus* mIL12, $P < .0001$.

Tumor vascularity and VEGF expression were decreased by treatment with individual armed viruses and even more by the combination of G47Δ-mAngio with G47Δ-mIl12 (Figure 7). G47Δ-Empty infection was accompanied by the presence of dense active macrophages, whereas the areas of G47Δ-mAngio or G47Δ-mIL12 infection were characterized by necrosis and decreased macrophage density compared to G47Δ-Empty. The combination of G47Δ-mAngio with G47Δ-mIL12 not only resulted in a large decrease in vascularity (CD31), VEGF (Figure 7*A*), and EGFR expression (Figure 6) but also abrogated the infiltration of mature macrophages (F4/80) seen with G47Δ-Empty infection (Figure 7*A*). Therefore, increased efficacy of combined G47Δ-mAngio plus G47Δ-mIL12 treatment was associated with decreases in both tumor vascularity and macrophage infiltration, which may have facilitated virus spread. The expression of VEGF and CD31 in different groups were quantified (Figure 7*B*).

Discussion

We provide evidence that treatment of GBM with oHSVs expressing IL-12 and angiostatin can improve outcomes. Indeed, combining two oHSVs, one expressing IL-12 and the other angiostatin, increases survival of animals bearing either of two different models of human GBM, and increased antiangiogenesis induced by the combination of IL-12 and angiostatin was observed *in vitro* and *in vivo*. This is in agreement with previously published data showing IL-12 as a mediator of the angiostatin-initiated antiangiogenic pathway [28,29]. Immunohistologic analysis of tissues after treatment has provided information on the cellular and molecular mechanisms underlying this therapy: 1) treatment with G47Δ-mIL12 + G47Δ-mAngio decreases expression of angiogenic markers (CD31 and VEGF) and $CD31^+$ vessels to a greater degree than either virus alone, thus confirming the improved antiangiogenic effect of combining viruses expressing these two molecules [28,29]; 2) decreased angiogenesis corresponds with a decrease of macrophage infiltration as previously described [12,19], which results in 3) increased intratumoral viral spread [10,11].

For this study, we have selected two highly angiogenic tumors because angiogenesis is a primary target of the treatment. Less angiogenic tumors may be less responsive to the treatment, but this would be a concern only on a limited subgroup of GBM since angiogenesis is a very common feature of GBMs. The combination of two viruses expressing mAngio and mIL-12 led to a greater therapeutic effect in U87 tumors than in MGG4. This is probably due to the fact that U87 cells are more permissive to G47Δ replication and thus express higher amounts of the transgenic cytokines (data not shown). Indeed, when taken individually, each virus showed a better therapeutic effect in U87 cells than in MGG4 GSCs.

The use of oncolytic viruses expressing antiangiogenic factors for tumor treatment has been previously described [8,16]. However, only more recently, studies have shown that decreased angiogenesis not only prevents tumor growth but also allows increased lysis of tumor cells by the viruses, thus emphasizing the importance of combining these two therapeutic strategies [12,17–19]. Herein, we have expanded this concept by combining oHSVs expressing two different antiangiogenic factors, one of which (IL-12) is a mediator of the activity of the other (angiostatin).

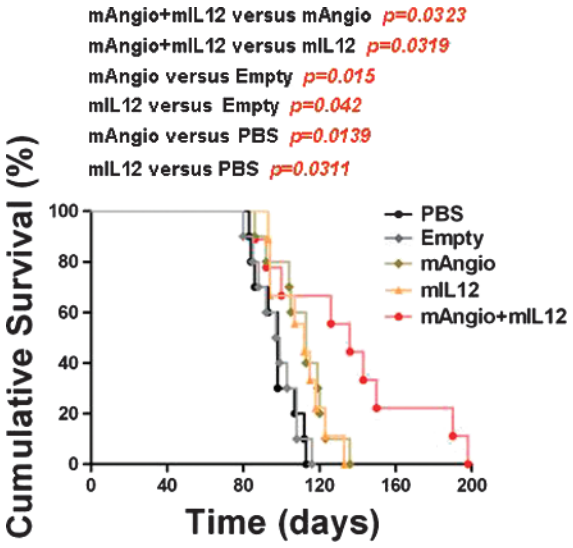

Figure 5. Kaplan-Meier analysis of survival after combination treatment of MGG4 GBM. Survival of mice ($n = 10$/group) with established MGG4 intracranial tumors and treated with PBS (median survival = 98 days), G47Δ-Empty (Empty; 98 days), G47Δ-mAngio (mAngio; 113 days), G47Δ-mIL12 (mIL12; 112 days), and G47Δ-mAngio + G47Δ-mIL12 (mAngio + mIL12; 136 days). The *P* values for each pairwise comparison are indicated.

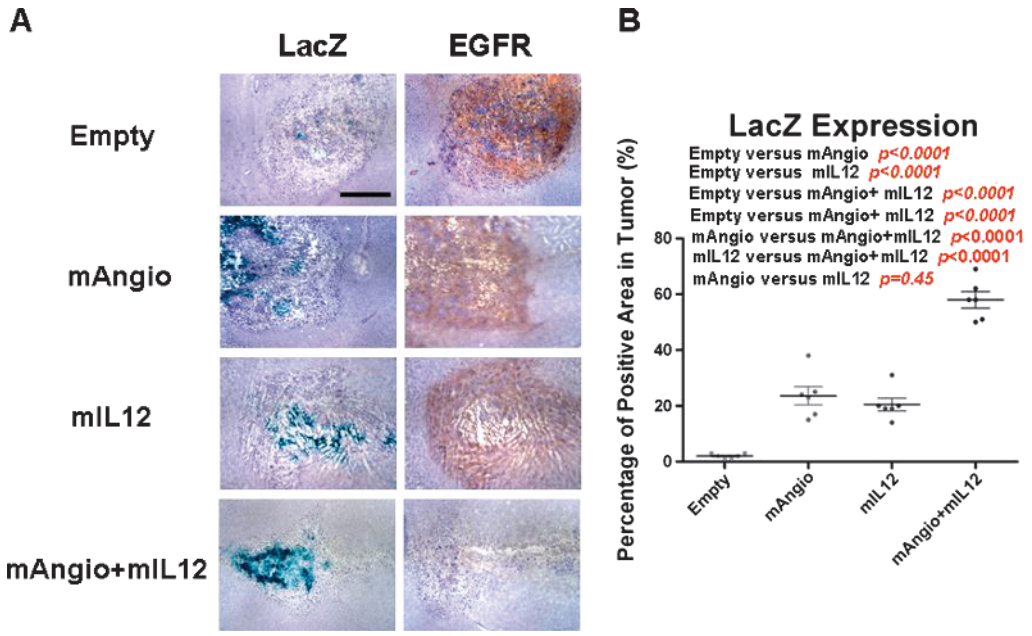

Figure 6. Virus infection of intracranial MGG4 tumors. (A) Nude mice with established intracranial MGG4 tumors were treated with intratumoral injection of G47Δ-Empty (Empty), G47Δ-mAngio (mAngio), G47Δ-mIL12 (mIL12), and G47Δ-mAngio + G47Δ-mIL12 (mAngio + mIL12; $n = 3$/group) and sacrificed 3 days later. Sections of the central tumor show viral distribution [viral β-galactosidase activity (LacZ), blue] and tumor cells (EGFR, brown). The bar indicates 2 mm. (B) Quantification of LacZ staining in the tumor area. Six dots per group represent six different fields in three different tumors (two fields per tumor). The percentage of positive areas in tumor is calculated as LacZ-positive areas/EGFR-positive areas × 100 (%). The bars indicate the average percentage of positive areas from six independent fields.

Interestingly, IL-12 was shown to induce immune responses in preclinical models of GBM and other malignancies, when delivered through oHSV vectors [37–44]. This may seem in contrast with the inhibition of macrophage infiltration that we observe. However, such differences may be due to the occurrence of different immune responses at different times following an inflammatory stimulus. In this respect, we tested the tissues at 3 days following oHSV injection, a time of acute inflammation in response to the virus. IL-12–induced immunity against the cancer would be expected to be observed at later time points. In addition, because these experiments were done with athymic mice, we could not determine whether there was establishment of adaptive antitumor immune responses. It may be that the integral immune system of an

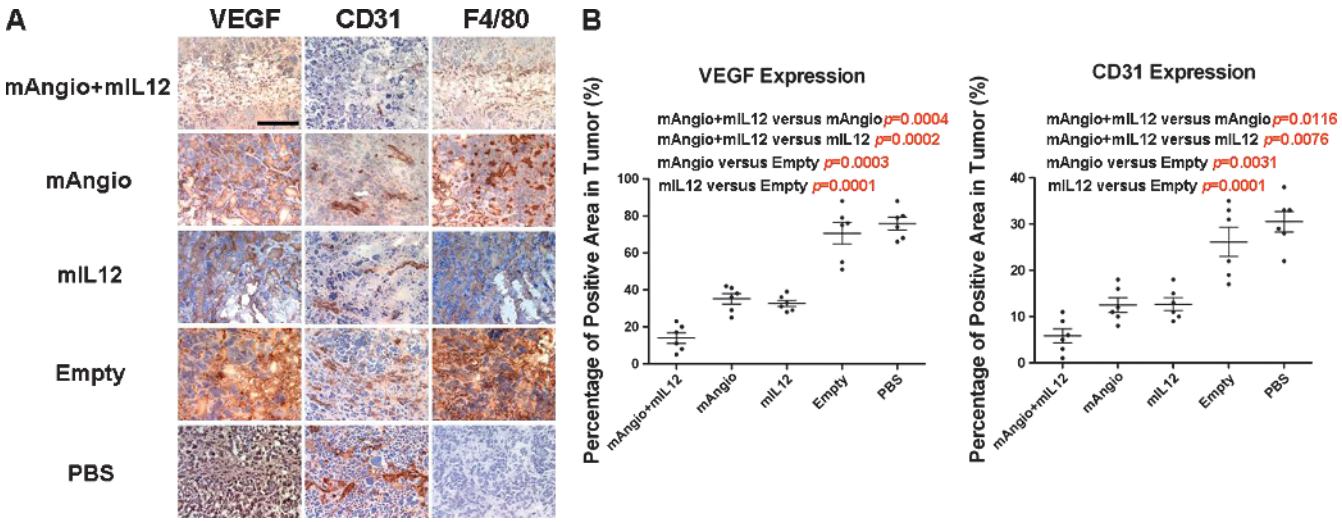

Figure 7. Immunohistochemical analysis of tumors. (A) Tumors were intratumorally injected with G47Δ-mAngio + G47Δ-mIL12 (mAngio + IL-12), G47Δ-mAngio, G47Δ-mIL12, G47Δ-Empty, or PBS ($n = 3$/group) and sacrificed 3 days later. Sections of the central tumor area showing VEGF expression (VEGF, diffuse brown staining of the secreted molecule), tumor vascularity (CD31, brown), and macrophage infiltration (F4/80, brown) in adjacent sections. The bar indicates 0.5 mm. (B) Quantification of VEGF and CD31 expression in different groups. The percentage of positive areas in tumor is defined as the percentage of VEGF or CD31-positive areas per field. The *P* values are indicated.

immunocompetent model will limit increased viral replication in the presence of excessive IL-12. Further characterization of this therapy requires detailed testing in an immunocompetent mouse model and analysis of potential establishment of anticancer immunity.

Overall, these data demonstrate the ability of oHSV-induced combinatorial antiangiogenic therapy to improve the efficacy of human GBM treatment and suggest that further studies are indicated with a goal toward clinical translation.

References

[1] Louis DN, Pomeroy SL, and Cairncross JG (2002). Focus on central nervous system neoplasia. *Cancer Cell* **1**, 125–128.

[2] Martuza RL, Malick A, Markert JM, Ruffner KL, and Coen DM (1991). Experimental therapy of human glioma by means of a genetically engineered virus mutant. *Science* **252**, 854–856.

[3] Fulci G and Chiocca EA (2003). Oncolytic viruses for the therapy of brain tumors and other solid malignancies: a review. *Front Biosci* **8**, e346–e360.

[4] Aghi M, Rabkin S, and Martuza RL (2006). Effect of chemotherapy-induced DNA repair on oncolytic herpes simplex viral replication. *J Natl Cancer Inst* **98**, 38–50.

[5] Liu TC, Castelo-Branco P, Rabkin SD, and Martuza RL (2008). Trichostatin A and oncolytic HSV combination therapy shows enhanced antitumoral and antiangiogenic effects. *Mol Ther* **16**, 1041–1047.

[6] Post DE, Fulci G, Chiocca EA, and Van Meir EG (2004). Replicative oncolytic herpes simplex viruses in combination cancer therapies. *Curr Gene Ther* **4**, 41–51.

[7] Kanai R, Wakimoto H, Cheema T, and Rabkin SD (2010). Oncolytic herpes simplex virus vectors and chemotherapy: are combinatorial strategies more effective for cancer? *Future Oncol* **6**, 619–634.

[8] Kaur B, Cripe TP, and Chiocca EA (2009). "Buy one get one free": armed viruses for the treatment of cancer cells and their microenvironment. *Curr Gene Ther* **9**, 341–355.

[9] Friedman A, Tian JP, Fulci G, Chiocca EA, and Wang J (2006). Glioma virotherapy: effects of innate immune suppression and increased viral replication capacity. *Cancer Res* **66**, 2314–2319.

[10] Fulci G, Breymann L, Gianni D, Kurozomi K, Rhee SS, Yu J, Kaur B, Louis DN, Weissleder R, Caligiuri MA, et al. (2006). Cyclophosphamide enhances glioma virotherapy by inhibiting innate immune responses. *Proc Natl Acad Sci USA* **103**, 12873–12878.

[11] Fulci G, Dmitrieva N, Gianni D, Fontana EJ, Pan X, Lu Y, Kaufman CS, Kaur B, Lawler SE, Lee RJ, et al. (2007). Depletion of peripheral macrophages and brain microglia increases brain tumor titers of oncolytic viruses. *Cancer Res* **67**, 9398–9406.

[12] Kurozumi K, Hardcastle J, Thakur R, Yang M, Christoforidis G, Fulci G, Hochberg FH, Weissleder R, Carson W, Chiocca EA, et al. (2007). Effect of tumor microenvironment modulation on the efficacy of oncolytic virus therapy. *J Natl Cancer Inst* **99**, 1768–1781.

[13] Lamfers ML, Fulci G, Gianni D, Tang Y, Kurozumi K, Kaur B, Moeniralm S, Saeki Y, Carette JE, Weissleder R, et al. (2006). Cyclophosphamide increases transgene expression mediated by an oncolytic adenovirus in glioma-bearing mice monitored by bioluminescence imaging. *Mol Ther* **14**, 779–788.

[14] Seystahl K, Wiestler B, Hundsberger T, Happold C, Wick W, Weller M, and Wick A (2013). Bevacizumab alone or in combination with irinotecan in recurrent WHO grade II and grade III gliomas. *Eur Neurol* **69**, 95–101.

[15] Piccioni D, Lai A, Nghiemphu P, and Cloughesy T (2012). Bevacizumab as first-line therapy for glioblastoma. *Future Oncol* **8**, 929–938.

[16] Tysome JR, Lemoine NR, and Wang Y (2009). Combination of anti-angiogenic therapy and virotherapy: arming oncolytic viruses with anti-angiogenic genes. *Curr Opin Mol Ther* **11**, 664–669.

[17] Libertini S, Iacuzzo I, Perruolo G, Scala S, Ierano C, Franco R, Hallden G, and Portella G (2008). Bevacizumab increases viral distribution in human anaplastic thyroid carcinoma xenografts and enhances the effects of E1A-defective adenovirus dl922-947. *Clin Cancer Res* **14**, 6505–6514.

[18] Otsuki A, Patel A, Kasai K, Suzuki M, Kurozumi K, Chiocca EA, and Saeki Y (2008). Histone deacetylase inhibitors augment antitumor efficacy of herpes-based oncolytic viruses. *Mol Ther* **16**, 1546–1555.

[19] Zhang W, Fulci G, Buhrman JS, Stemmer-Rachamimov AO, Chen JW, Wojtkiewicz GR, Weissleder R, Rabkin SD, and Martuza RL (2011). Bevacizumab with angiostatin-armed oHSV increases antiangiogenesis and decreases bevacizumab-induced invasion in U87 glioma. *Mol Ther* **20**, 37–45.

[20] O'Reilly MS, Holmgren L, Shing Y, Chen C, Rosenthal RA, Moses M, Lane WS, Cao Y, Sage EH, and Folkman J (1994). Angiostatin: a novel angiogenesis inhibitor that mediates the suppression of metastases by a Lewis lung carcinoma. *Cell* **79**, 315–328.

[21] Dell'Eva R, Pfeffer U, Indraccolo S, Albini A, and Noonan D (2002). Inhibition of tumor angiogenesis by angiostatin: from recombinant protein to gene therapy. *Endothelium* **9**, 3–10.

[22] Perri SR, Annabi B, and Galipeau J (2007). Angiostatin inhibits monocyte/macrophage migration via disruption of actin cytoskeleton. *FASEB J* **21**, 3928–3936.

[23] Stack MS, Gately S, Bafetti LM, Enghild JJ, and Soff GA (1999). Angiostatin inhibits endothelial and melanoma cellular invasion by blocking matrix-enhanced plasminogen activation. *Biochem J* **340**(pt 1), 77–84.

[24] Kirsch M, Strasser J, Allende R, Bello L, Zhang J, and Black PM (1998). Angiostatin suppresses malignant glioma growth *in vivo*. *Cancer Res* **58**, 4654–4659.

[25] Wahl ML, Moser TL, and Pizzo SV (2004). Angiostatin and anti-angiogenic therapy in human disease. *Recent Prog Horm Res* **59**, 73–104.

[26] Ma HI, Lin SZ, Chiang YH, Li J, Chen SL, Tsao YP, and Xiao X (2002). Intratumoral gene therapy of malignant brain tumor in a rat model with angiostatin delivered by adeno-associated viral (AAV) vector. *Gene Ther* **9**, 2–11.

[27] Wong RJ, Chan MK, Yu Z, Ghossein RA, Ngai I, Adusumilli PS, Stiles BM, Shah JP, Singh B, and Fong Y (2004). Angiogenesis inhibition by an oncolytic herpes virus expressing interleukin 12. *Clin Cancer Res* **10**, 4509–4516.

[28] Albini A, Brigati C, Ventura A, Lorusso G, Pinter M, Morini M, Mancino A, Sica A, and Noonan DM (2009). Angiostatin anti-angiogenesis requires IL-12: the innate immune system as a key target. *J Transl Med* **7**, 5.

[29] Gyorffy S, Palmer K, Podor TJ, Hitt M, and Gauldie J (2001). Combined treatment of a murine breast cancer model with type 5 adenovirus vectors expressing murine angiostatin and IL-12: a role for combined anti-angiogenesis and immunotherapy. *J Immunol* **166**, 6212–6217.

[30] Todo T, Martuza RL, Rabkin SD, and Johnson PA (2001). Oncolytic herpes simplex virus vector with enhanced MHC class I presentation and tumor cell killing. *Proc Natl Acad Sci USA* **98**, 6396–6401.

[31] Todo, T (2009). A clinical study of a replication-competent, recombinant herpes simplex virus type 1 (G47delta) in patients with progressive glioblastoma. http://appswhoint/trialsearch/trialaspx?trialid=JPRN-UMIN000002661; Japan Primary Registries Network (Internet), Wako-shi (Saitama), National Institute of Public Health (Japan). 2008 Oct 16. Identifier JPRN-UMIN000002661.

[32] Wakimoto H, Kesari S, Farrell CJ, Curry WT Jr, Zaupa C, Aghi M, Kuroda T, Stemmer-Rachamimov A, Shah K, Liu TC, et al. (2009). Human glioblastoma-derived cancer stem cells: establishment of invasive glioma models and treatment with oncolytic herpes simplex virus vectors. *Cancer Res* **69**, 3472–3481.

[33] Wakimoto H, Mohapatra G, Kanai R, Curry WT Jr, Yip S, Nitta M, Patel AP, Barnard ZR, Stemmer-Rachamimov AO, Louis DN, et al. (2011). Maintenance of primary tumor phenotype and genotype in glioblastoma stem cells. *Neuro Oncol* **14**, 132–144.

[34] Pandita A, Aldape KD, Zadeh G, Guha A, and James CD (2004). Contrasting *in vivo* and *in vitro* fates of glioblastoma cell subpopulations with amplified EGFR. *Genes Chromosomes Cancer* **39**, 29–36.

[35] Wong RJ, Patel SG, Kim S, DeMatteo RP, Malhotra S, Bennett JJ, St-Louis M, Shah JP, Johnson PA, and Fong Y (2001). Cytokine gene transfer enhances herpes oncolytic therapy in murine squamous cell carcinoma. *Hum Gene Ther* **12**, 253–265.

[36] Kuroda T, Martuza RL, Todo T, and Rabkin SD (2006). Flip-Flop HSV-BAC: bacterial artificial chromosome based system for rapid generation of recombinant herpes simplex virus vectors using two independent site-specific recombinases. *BMC Biotechnol* **6**, 40.

[37] Hellums EK, Markert JM, Parker JN, He B, Perbal B, Roizman B, Whitley RJ, Langford CP, Bharara S, and Gillespie GY (2005). Increased efficacy of an interleukin-12-secreting herpes simplex virus in a syngeneic intracranial murine glioma model. *Neuro Oncol* **7**, 213–224.

[38] Parker JN, Gillespie GY, Love CE, Randall S, Whitley RJ, and Markert JM (2000). Engineered herpes simplex virus expressing IL-12 in the treatment of experimental murine brain tumors. *Proc Natl Acad Sci USA* **97**, 2208–2213.

[39] Parker JN, Meleth S, Hughes KB, Gillespie GY, Whitley RJ, and Markert JM (2005). Enhanced inhibition of syngeneic murine tumors by combinatorial therapy with genetically engineered HSV-1 expressing CCL2 and IL-12. *Cancer Gene Ther* **12**, 359–368.

[40] Parker JN, Pfister LA, Quenelle D, Gillespie GY, Markert JM, Kern ER, and Whitley RJ (2006). Genetically engineered herpes simplex viruses that express IL-12 or GM-CSF as vaccine candidates. *Vaccine* **24**, 1644–1652.

[41] Toda M, Martuza RL, Kojima H, and Rabkin SD (1998). *In situ* cancer vaccination: an IL-12 defective vector/replication-competent herpes simplex virus combination induces local and systemic antitumor activity. *J Immunol* **160**, 4457–4464.

[42] Varghese S, Rabkin SD, Liu R, Nielsen PG, Ipe T, and Martuza RL (2006). Enhanced therapeutic efficacy of IL-12, but not GM-CSF, expressing oncolytic herpes simplex virus for transgenic mouse derived prostate cancers. *Cancer Gene Ther* **13**, 253–265.

[43] Varghese S, Rabkin SD, Nielsen PG, Wang W, and Martuza RL (2006). Systemic oncolytic herpes virus therapy of poorly immunogenic prostate cancer metastatic to lung. *Clin Cancer Res* **12**, 2919–2927.

[44] Ino Y, Saeki Y, Fukuhara H, and Todo T (2006). Triple combination of oncolytic herpes simplex virus-1 vectors armed with interleukin-12, interleukin-18, or soluble B7-1 results in enhanced antitumor efficacy. *Clin Cancer Res* **12**, 643–652.